Drug Design, Development and Therapy

Dovepress
open access to scientific and medical research

Open Access Full Text Article

ORIGINAL RESEARCH

# MicroRNA-664 suppresses the growth of cervical cancer cells via targeting c-Kit

This article was published in the following Dove Press journal:
*Drug Design, Development and Therapy*



Mingfen Lv[1,2]
Rongying Ou[3]
Qianwen Zhang[1]
Fan Lin[1]
Xiangyun Li[4]
Keyu Wang[2]
Yunsheng Xu[1,4]

[1]Department of Dermatology, The First Affiliated Hospital of Wenzhou Medical University, Wenzhou, Zhejiang 325000, People's Republic of China; [2]Department of Dermatology, Qilu Hospital, Shandong University, Jinan, Shandong 250012, People's Republic of China; [3]Department of Gynaecology and Obstetrics, The First Affiliated Hospital of Wenzhou Medical University, Wenzhou, Zhejiang 325000, People's Republic of China; [4]Department of Dermatology, The Seventh Affiliated Hospital of Sun Yat-sen university, Shenzhen, Guangdong 518107, People's Republic of China

**Background:** Cervical cancer is the second most common malignant cancer in women worldwide. Evidence indicated that miR-664 was significantly downregulated in cervical cancer. However, the mechanisms by which miR-664 regulates the tumorigenesis of cervical cancer remain unclear. Thus, this study aimed to investigate the role of miR-664 in cervical cancer.

**Methods:** Quantitative reverse transcription polymerase chain reaction was used to detect the level of miR-664 in tumor tissues and cell line. The dual luciferase reporter system assay and Western blotting were used to explore the interaction of miR-664 and c-Kit in cervical cancer.

**Results:** The expression of miR-664 in patients with cervical cancer was dramatically decreased compared with that in adjacent tissues. MiR-664 mimics significantly inhibited proliferation in SiHa cells via inducing apoptosis. In addition, miR-664 mimics induced apoptosis in SiHa cells via increasing the expressions of Bax and active caspase 3 and decreasing the level of Bcl-2. Moreover, dual-luciferase assay showed that c-Kit was the directly binding target of miR-664 in SiHa cells; overexpression of miR-664 downregulated the expression of c-Kit. Meanwhile, upregulation of miR-664 significantly decreased the levels of c-Myc and Cyclin D in cells. Furthermore, miR-664 markedly inhibited tumor growth of cervical cancer in xenograft.

**Conclusion:** Our data indicated that miR-664 exerted antitumor effects on SiHa cells by directly targeting c-Kit in vitro and in vivo. Therefore, miR-664 might be a potential therapeutic target for the treatment of patients with cervical cancer.

**Keywords:** microRNA-664, c-Kit, cervical cancer, apoptosis

## Introduction

Cervical cancer is the second most common kind of cancer, which causes severe harm to the health of women worldwide.[1] Cervical cancer has a high morbidity and mortality worldwide causing more than 470,000 new cases and 300,000 deaths every year.[1] High-risk human papilloma virus (HR-HPV) is the main nosogenesis in the development of cervical cancer.[2] In addition, HPV is associated with the abnormal expressions of multiple genes and cellular microRNAs in cervical cancer.[3,4] Despite surgery and chemotherapy that were commonly used in the treatment of cervical cancer, the 5-year overall survival rate of patients still remains poor.[5] Therefore, in this study, we investigated the molecular mechanisms in genesis in order to develop a new treatment strategy for patients with cervical cancer.

miRNAs are a sizable kind of small noncoding RNAs of 18–25 nucleotides.[6,7] Through binding the 3′-untranslated regions (3′-UTRs) of the target mRNA to regulate gene expression.[8,9] Previous studies have indicated that miRNAs participate in mediating multiple biological processes, such as cell proliferation, apoptosis

Correspondence: Keyu Wang
Department of Dermatology, Qilu Hospital, Shandong University, No. 107 Wenhua West Road, Jinan, Jinan 250012, People's Republic of China
Email keyuwang101@hotmail.com

Yunsheng Xu
Department of Dermatology, The First Affiliated Hospital of Wenzhou Medical University, Shangcai Village, Nanbaixiang Street, Ouhai District, Wenzhou, Zhejiang 325000, People's Republic of China
Email xuyunsheng1018@163.com

submit your manuscript | www.dovepress.com
DovePress
http://doi.org/10.2147/DDDT.S203399

and invasion.[10,11] Previous studies indicated that several miRNAs could regulate cell growth in cervical cancer cells.[12,13] miR-664 is a member of the microRNA family.[14,15] Previous studies reported that miR-664 could regulate apoptosis, migration and invasion in various tumor cells.[16,17] Yang et al found that miR-664 could inhibit cell growth in cervical cancer.[18] However, the mechanisms by which miR-664 regulates the tumorigenesis of cervical cancer remain unclear.

Stem cell factor receptor c-Kit, a proto-oncogene, encodes a transmembrane kinase.[19,20] C-Kit plays an important role in tumor growth and apoptosis on gastrointestinal stromal tumor, melanoma and myeloma.[21,22] Previous studies reported that c-Kit could regulate cell proliferation and apoptosis in cervical cancer.[23,24] Although there are some reports about miR-664 and c-Kit, the interaction between miR-664 and c-Kit in cervical cancer remains unclear. In this study, we aimed to investigate the role of miR-664 and c-Kit in cervical cancer.

# Materials and methods

## Clinical specimens

Thirty pairs of cervical cancer samples and adjacent normal tissues were collected between May 2017 and April 2018 from the First Affiliated Hospital of Wenzhou Medical University. All the study subjects were aged from 30 to 45 years. Clinical and pathological data of these patients were collected with their written informed consents. Patients gave consent to their tissues being used for research purposes. And the patients gave written informed consent. The present study was approved by the Ethics Committee of The First Affiliated Hospital of Wenzhou Medical University.

## Cell culture

The human cervical cancer cell line SiHa was purchased from American Type Culture Collection (Rockville, MD, USA). The cells were maintained in DMEM and supplemented with 10% FBS (Invitrogen, Carlsbad, CA, USA), and 1% penicillin and streptomycin (100 U/mL) in a humidified atmosphere of 5% $CO_2$ incubator at 37°C.

## Quantitative reverse transcription polymerase chain reaction (qRT-PCR)

The total RNAs were extracted using the RNA extraction kit (TaKaRa Bio Inc. Shiga, Japan) according to the manufacturer's instructions. cDNA was synthesized using the RNA PCR Kit (TaKaRa, Ver.3.0) according to the manufacturer's instructions. Real-time PCR was performed as follows: firstly, 94°C for 2 mins, followed by 35 cycles of 94°C for 30 s, 55°C for 45 s. PCRs were carried out using SYBR premix Ex Taq II kit (TaKaRa) on an ABI 7500 Real-Time PCR system (ABI, NY, USA). The primers for miR-664 were purchased from GenePharma (Shanghai, China). miR-664: forward, 5' -GAGAGAAGGCCUCCCUAGCCAGC −3' and reverse, 5' -ACUGGCUAGGGAAAAUGAUUGGAU-3'. GAPDH: forward, 5' – ATGGCCTTCCGTGTTCCTAC-3'; reverse, 5'-CTTTACAAAGTTGTCGTTGA-3'. All samples were performed in triplicates. Relative quantification of gene expression was calculated using the $2^{-\Delta\Delta CT}$ method.

## MiR-664 mimics transfection

MiR-664 mimics or mimics control were provided by GenePharma (Shanghai, China). SiHa cells were seed into 6-well plate and cultured for 24 hrs. Upon reaching 80% confluence, cells in serum-free medium were transfected with miR-664 mimics and mimics control using 5 μL Lipofectamine® 2,000 transfection reagent (Invitrogen; Thermo Fisher Scientific, Inc.). The final concentration of mimics used was 10 nM and the transfection period was 6 hrs. Then, a medium containing 10% FBS was added into each well to terminate reaction at 37°C. After incubated for 48 hrs, cells were collected for subsequent analyses.

## Cell counting kit-8 (CCK-8) assay

Cell viability was determined using the CCK-8 (Beyotime Institute of Biotechnology, Haimen, China) according to the manufacturer's protocols. SiHa cells ($5\times10^3$ cells/well) were plated in a 96-well plate overnight at 37°C. Upon reaching 80% confluence, cells were transfected with miR-664 mimics or mimics control (NC) for 6 hrs at 37°C. After 48-hr incubation, 10 μL CCK-8 reagent was added to each well and then incubated for 2 hrs. The absorbance values were measured at 450 nm wavelength (Bio-Rad Laboratories, Benicia, California, USA).

## Immunofluorescence

SiHa cells were plated in 24-well plates overnight at 37°C. Upon reaching 80% confluence, cells were transfected with miR-664 mimics or mimics control (NC) for 6 hrs at 37°C. After 48-hr incubation, cells were washed in PBS three times and fixed in 4% paraformaldehyde for 20 mins at room temperature. The cells were then fixed in pre-cold methanol for 10 mins at −20°C, followed by incubation with primary antibodies for anti-Ki67

(Abcam; ab15580) (1:1000), DAPI (ab104139) at 4°C overnight. After being washed 3 times with PBS, cells were incubated with secondary antibodies (Abcam; ab150080) (1:5000) at 37°C for 1 hr. The samples were observed by fluorescence microscope at once (Olympus CX23 Tokyo, Japan).

## Flow cytometric analysis of cell apoptosis

SiHa cells were plated in 24-well plates overnight at 37°C. Upon reaching 80% confluence, cells were transfected with miR-664 mimics or mimics control (NC) for 6 hrs at 37°C. After 48-hr incubation, the cells were washed 3 times with pre-cold PBS. Then, cells were resuspended with 100 μL binding buffer. Later on, 5 μL Annexin V-FITC and 5 μL propidium were added. After 15 mins of incubation at room temperature, 400 μL binding buffer was added to each sample. The cell apoptosis was measured by flow-cytometer (BD, Franklin Lake, NJ, USA) and quantified with the Cellquest software.

## Western blot analysis

SiHa cells were lysed in cell RIPA buffer (Thermo Fisher Scientific, Waltham, MA, USA). Bradford Protein Assay Kit (Beyotime) was used to measure the protein concentration. Then, an equal amount of protein was separated using 10% SDS polyacrylamide gel and transported onto polyvinylidene fluoride membranes (PVDF, Thermo) in 2 h. The PVDF membranes were blocked in 5% non-fat milk in TBST at room temperature for 1 h. Later on, the membranes were washed in TBST 3 times and incubated with primary antibodies overnight at 4 °C: anti-Bax (Abcam; ab32503) (1:1000), anti-Bcl-2 (Abcam; ab32124) (1:1000), anti-active caspase 3 (Abcam; ab2302) (1:1000), anti-c-Kit (Abcam; ab216450) (1:1000), anti-c-myc (Abcam; ab32072) (1:1000), anti-cyclin D1 (Abcam; ab16663) (1:1000), anti-β-actin (Abcam; ab8227) (1:1000), After washing with TBST for three times, the membrane was incubated with secondary antibody goat anti-mouse IgG secondary antibody (Abcam; ab6789) (1:5000), goat anti-rabbit IgG secondary antibody (Abcam; ab205718) (1:5000) before determined by chemiluminescence. Finally, the PVDF membranes were incubated with ECL reagent (Santa Cruz Biotechnology) to detect the blots. The density of blots for proteins were normalized to β-actin.

## Cell migration assay

SiHa cells were transfected as described previously. The transfected cells ($1\times10^5$ cells/well) were seeded into the upper chamber (8 μm, Corning Inc., Corning, NY, USA) in 300 μL serum-free medium. The lower chamber was contained 600 μL DMEM supplemented with 10% FBS. After 24-hr incubation, the cells on the upper surface of the membrane were removed with a cotton swab. Then, the migratory cells on the underside were stained with 0.1% crystal violet (Sigma Aldrich, St. Louis, MO, USA) for 1 hr. Finally, migratory cells were counted in five random fields under a microscope.

## The dual luciferase reporter system assay

The specific target *c-Kit* was searched, using three internet-based bioinformatics online website: TargetScan (www.targetscan.org), miRDB (www.mirdb.org) and microRNA (www.microRNA.org). The target gene sequence (WT) and the mutation gene sequence (MT) were designed and synthesized by GenePharma (Shanghai, China). The 3′-UTR region was then connected with the Xho I/Not I sites of the PsiCHECK2 vector (Promega, Madison, WI, USA). SiHa cells were co-transfected with 100 ng PsiCHECK2-c-Kit-WT or PsiCHECK2-c-Kit-MT and 100 nM miR-664 mimics or mimics control using lipo 2,000. Then, the cells were incubated in 5% $CO_2$ at 37°C, after fresh medium replaced the previous medium; the cells were transfected for 6 hrs. After 48-hr incubation, different groups of cells were digested by tritonX-100. The activities of firefly luciferase and renilla luciferase were measured by dual luciferase reporter assay system (Promega). The luminescent signals were analyzed by Tecan Infinite F200/M200 (Tecan, Männedorf, Switzerland) with the Gene5 software (BioTek).

## Animal study

To investigate the effects of miR-664 on the tumorigenicity of cervical cancer in vivo, 15 female BALB/nude mice (aged 4–6 weeks) were purchased from Shanghai Slac Animal Center (Shanghai, China). The nude mice were housed within a dedicated SPF facility and in a constant temperature of 20–23°C and 55–65% humidity. Fifteen nude mice were randomly divided into three groups (five per group): blank, NC and miR-664 mimics. SiHa cells ($6\times10^6$ cells) suspended in 100 μL PBS were injected subcutaneously into the right armpit flank of female athymic nude mice and 50 nM miR-664 mimics or NC was directly injected into the tumors twice a week when the tumors volumes reached to 180 $mm^3$. The tumor diameter was measured weekly. The tumor volume ($mm^3$) was measured and recorded according

to the equation (length × width$^2$)/2. All mice were euthanized at the end of the study using $CO_2$. Tumors were excised from mice and weighed. All animal experiments were performed in accordance with institutional guidelines, following a protocol approved by the Ethics Committees of The First Affiliated Hospital of Wenzhou Medical University.

## TUNEL staining

Deparaffinized tissue sections were stained using an APO-BrdU™ TUNEL Assay Kit (Thermo Fisher Scientific, Waltham, MA, USA, A23210), according to the manufacturer's instructions.

## Immunohistochemistry (IHC)

Tumor tissues isolated from mice were cut into 4-μm slices and embedded in paraffin. After being deparaffinized at 65°C for 2 hrs and 2.5-min antigen repair, slides were cooled for 1 hr at room temperature. Later on, sections were incubated with Ki67 primary antibody (ab15580, Abcam) at 4°C overnight. After that, the slides were incubated with secondary antibody (ab150077, Abcam). Ki67 staining was evaluated under a light microscope at 200 or 400× magnification.

## Statistical analysis

At least three independent experiments were performed for each group, and all values were expressed as the mean ± SD. The comparison between two groups was analyzed by Student's *t*-test. The comparisons among multiple groups were made with one-way ANOVA followed by Dunnett's test. For all tests, $P<0.05$ was considered to indicate a statistically significant difference.

# Results

## MiR-664 mimics inhibited the proliferation of SiHa cells

To determine the role of miR-664 in the development and progression of cervical cancer, the levels of miR-664 in cervical cancer tumor tissues and normal tissues were detected by qRT-PCR analysis. As shown in Figure 1A, the levels of miR-664 in cervical tumor tissues were significantly decreased compared with that in the normal tissues. To investigate the biological roles of miR-664 in cervical cancer, SiHa cells were transfected with miR-664 mimics or NC. As indicated in Figure 1B, the level of miR-664 was significantly upregulated in miR-664 mimics transfected cells, compared with NC. In addition, miR-664 mimics markedly inhibited the proliferation of SiHa cells

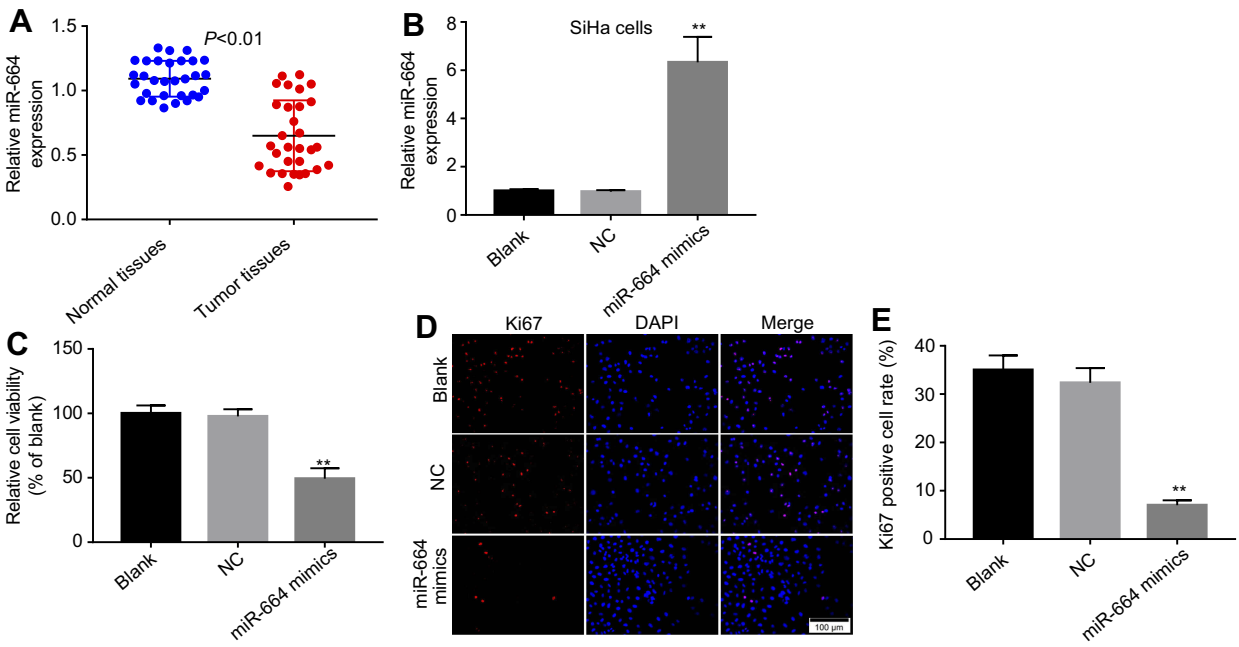


**Figure 1** MiR-664 mimics inhibited the proliferation of SiHa cells. (**A**) qRT-PCR was performed to examine the level of miR-664 in tissues samples between cervical cancer and control (**$P<0.01$ vs normal tissues). (**B**) SiHa cells were transfected with 10 nM miR-664 mimics or mimics NC for 6 hrs and incubated for another 48 hrs. The level of miR-664 was detected with qRT-PCR. (**C**) Cell viability in SiHa cells was determined using CCK-8 assay. (**D**) Relative fluorescence expression levels were quantified by Ki67 and DAPI staining. (**E**) The number of Ki67 positive cells were counted. **$P<0.01$ vs NC group.

(Figure 1C). Meanwhile, in immunofluorescence assays, the rates of Ki67 positive cells were notably decreased in miR-664 mimics transfected SiHa cells (Figure 1D). These results indicated that miR-664 could inhibit the proliferation of SiHa cells.

## MiR-664 mimics induced apoptosis of SiHa cells

Next, flow cytometric assay was used to detect the apoptosis of SiHa cells. As indicated in Figure 2A and B, miR-664 mimics significantly induced apoptosis in SiHa cells compared with the NC group. In addition, Western blotting was applied to detect the expressions of apoptosis-related proteins Bax, Bcl-2 and active caspase-3. The results showed that miR-664 mimics notably decreased the level of Bcl-2 and increased the expressions of Bax and active caspase 3 in cells (Figure 2C–F). All these data suggested that miR-664 could induce apoptosis of SiHa cells.

## MiR-664 mimics inhibited migration of SiHa cells

To further assess the effect of miR-664 on the migration of SiHa cells, transwell assay was applied. As shown in Figure 3A and B, miR-664 mimics significantly inhibited the migration ability of SiHa cells compared with the NC group. These data illustrated that miR-664 mimics could inhibit migration of SiHa cells.

## c-Kit is a direct binding target of miR-664

As demonstrated that miR-664 mimics inhibited the proliferation of SiHa cells via inducing apoptosis, we next investigated the potential direct binding target of miR-664. Online bioinformatics tools TargetScan, miRDB and microRNA were used to predict the downstream binding targets of miR-664. The data indicated that c-Kit was the possible molecular target of miR-664 (Figure 4A). Next, the dual luciferase reporter assay was used to confirm this result. As shown in Figure 4B, the luciferase activity was markedly downregulated following co-transfected with miR-664 mimics and psiCHECK-2-c-Kit-WT, while there was almost no change when the specific target was mutated. Based on this information, we determined that c-Kit was directly associated with miR-664. In addition, the results of Western blot indicated that the expressions of c-Kit, c-Myc and cyclin D were markedly decreased in cells treated with miR-664 mimics (Figure 4C–E). All these data illustrated that *c-Kit* was a direct binding target of miR-664.

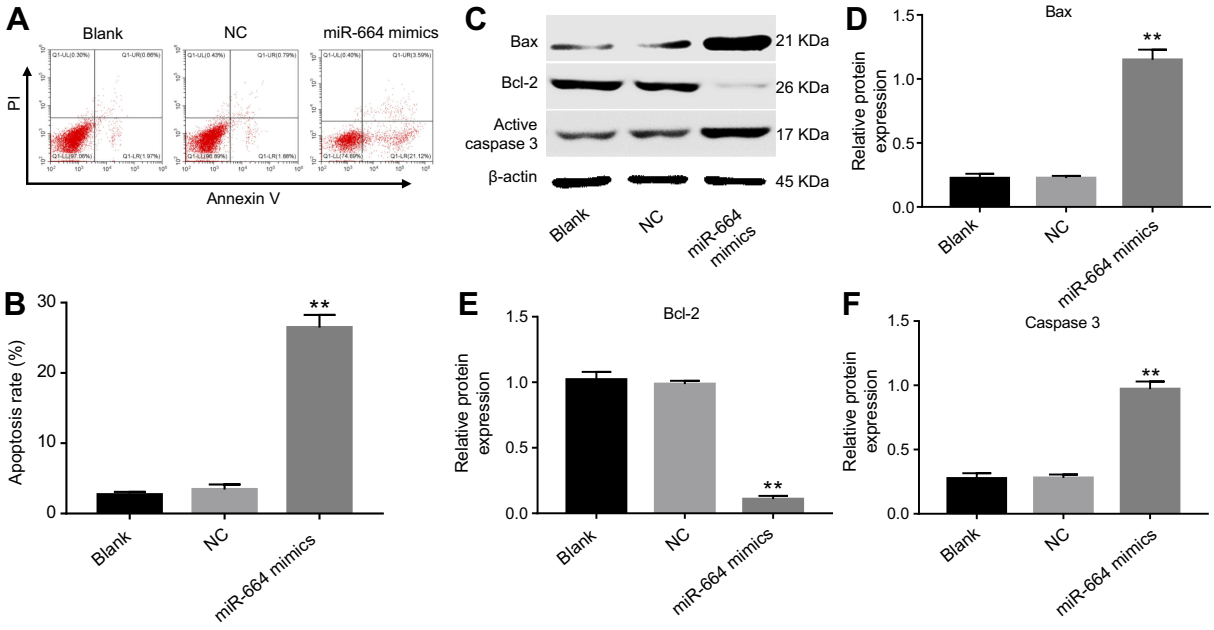


**Figure 2** MiR-664 mimics induced apoptosis of SiHa cells. SiHa cells were transfected with 10 nM miR-664 mimics or mimics NC for 6 hrs and incubated for another 48 hrs. (**A**) Apoptotic cells were detected with Annexin V and PI double staining. **(B)** The apoptosis cell rates were calculated. (**C**) The expressions of Bax, Bcl-2 and active caspase 3 in SiHa cells were analyzed by Western blotting. (**D**) The expression of Bax was quantified by normalizing to β-actin. (**E**) The expression of Bcl-2 was quantified by normalizing to β-actin. (**F**) The expression of active caspase 3 was quantified by normalizing to β-actin. $^{**}P<0.01$ vs NC group.

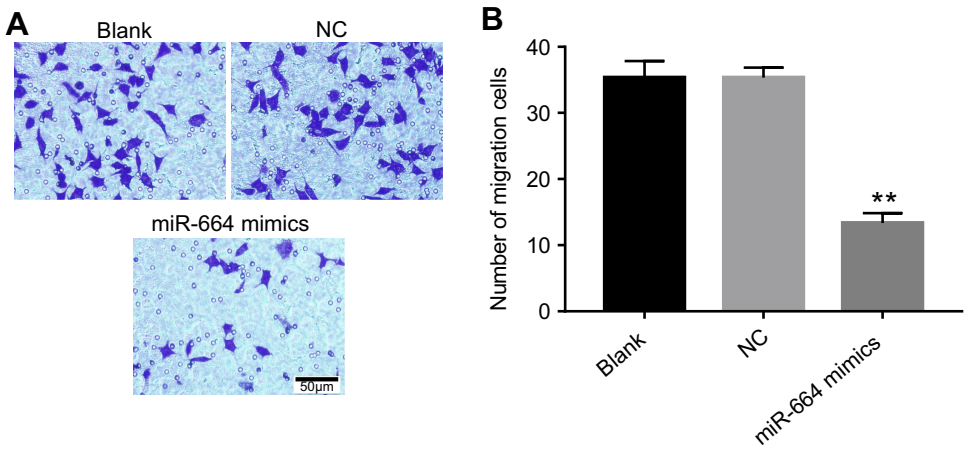


**Figure 3** MiR-664 mimics inhibited migration of SiHa cells. SiHa cells were transfected with 10 nM miR-664 mimics or mimics NC for 6 hrs and incubated for another 24 hrs. (**A**) The migration ability of U937 cells was examined using transwell migration assay. (**B**) The number of migration cells in each group was quantified. ***P*<0.01 vs NC group.

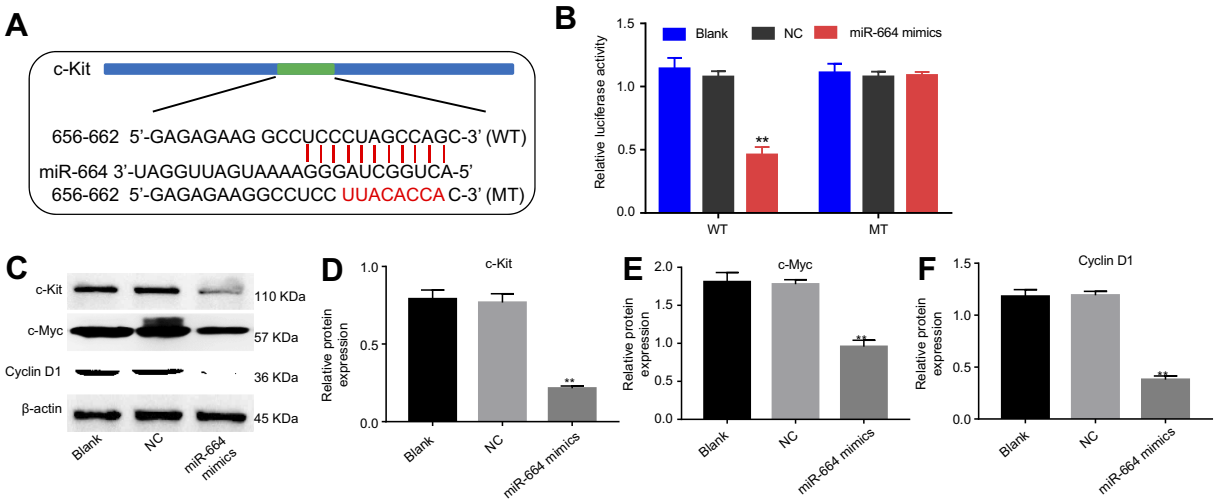


**Figure 4** *C-Kit* was a direct binding target of miR-664. (**A**) Gene structure of c-Kit at the position of 656–662 indicates the predicted target site of miR-664 in its 3'UTR, with a sequence of UCCCUAGCCAGC. (**B**) The luciferase activity was measured by using the dual luciferase reporter assay. (**C**) SiHa cells were transfected with 10 nM miR-664 mimics or mimics NC for 6 hrs and incubated for another 48 hes. The expressions of c-Kit, c-Myc and Cyclin D in SiHa cells were analyzed by Western blotting. (**D**) The expression of c-Kit was quantified by normalizing to β-actin. (**E**) The expression of c-Myc was quantified by normalizing to β-actin. (**F**) The expression of Cyclin D was quantified by normalizing to β-actin. ***P*<0.01 vs NC group.

## MiR-664 mimics exhibited antitumor effect on cervical cancer in vivo

To further confirm the effect of miR-664 on the growth of cervical cancer, a xenograft mouse model was used. As shown in Figure 5A and B, 50 nM miR-664 mimics significantly decreased the tumor volume, compared with the NC group. In addition, upregulation of miR-664 markedly reduced the weight of tumors (Figure 5C). Moreover, the data of TUNEL suggested that miR-664 mimics resulted in significant cell apoptosis in tumor tissues (Figure 5D and E). Meanwhile, IHC staining illustrated that the expression of Ki67 in tumor tissues was markedly decreased by the treatment of miR-664 mimics (Figure 5F and G). All these results indicated that miR-664 exhibited an antitumor effect on cervical cancer SiHa cells in vivo.

## MiR-664 mimics exhibited antitumor effects via induction apoptosis in vivo

We next examined the effects of miR-664 on the expression of apoptosis-related proteins in tumor tissues. As shown in Figure 6A, the level of miR-664 was significantly upregulated in tumor tissues injected with miR-664 mimics, compared with the NC group. Consistent with in vitro data, the expression of c-Kit was significantly decreased and the level of active caspase 3 was markedly increased in the miR-664 mimics group, compared with

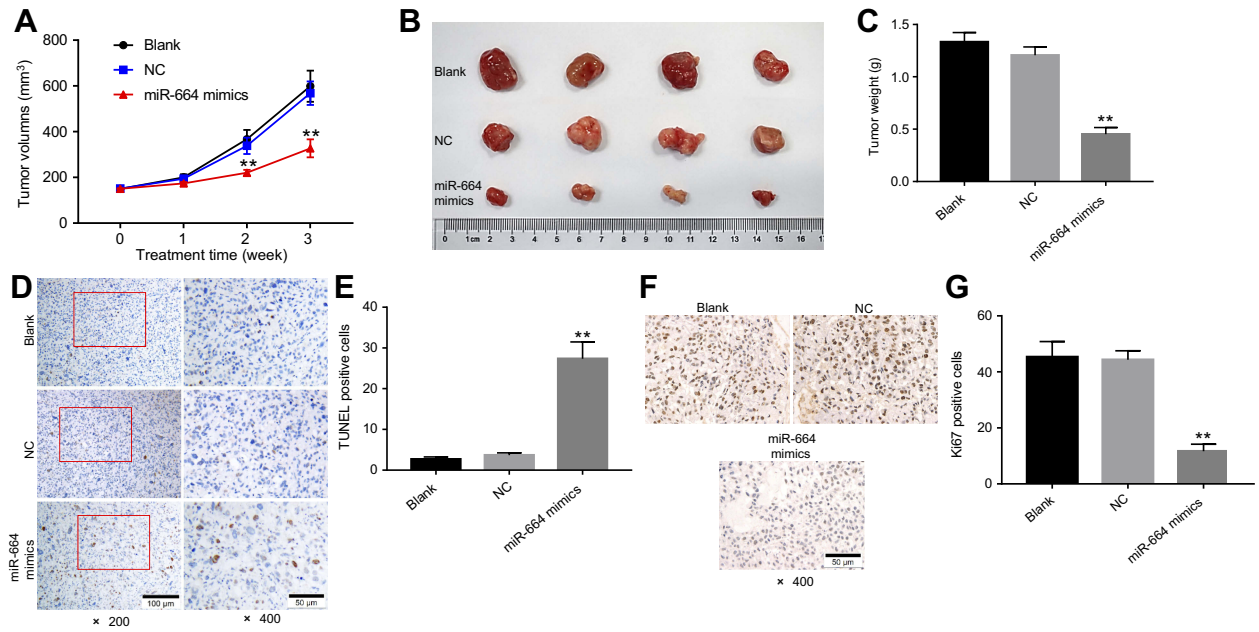


**Figure 5** MiR-664 mimics exhibited antitumor effects on cervical cancer in vivo. miR-664 mimics (50 nM) or NC was directly injected into the tumors twice a week. (**A**) Tumor volumes of mice were measured weekly post-inoculation of SiHa cells. (**B**) Tumors were isolated from xenografts and pictured at the end of study. (**C**) Tumor weights in each group were calculated. (**D** and **E**) TUNEL staining of tumor tissues in each group and TUNEL positive cell rate were calculated. (**F** and **G**) Relative fluorescence expression levels were quantified by Ki67 and DAPI staining. ***P*<0.01 vs NC group.

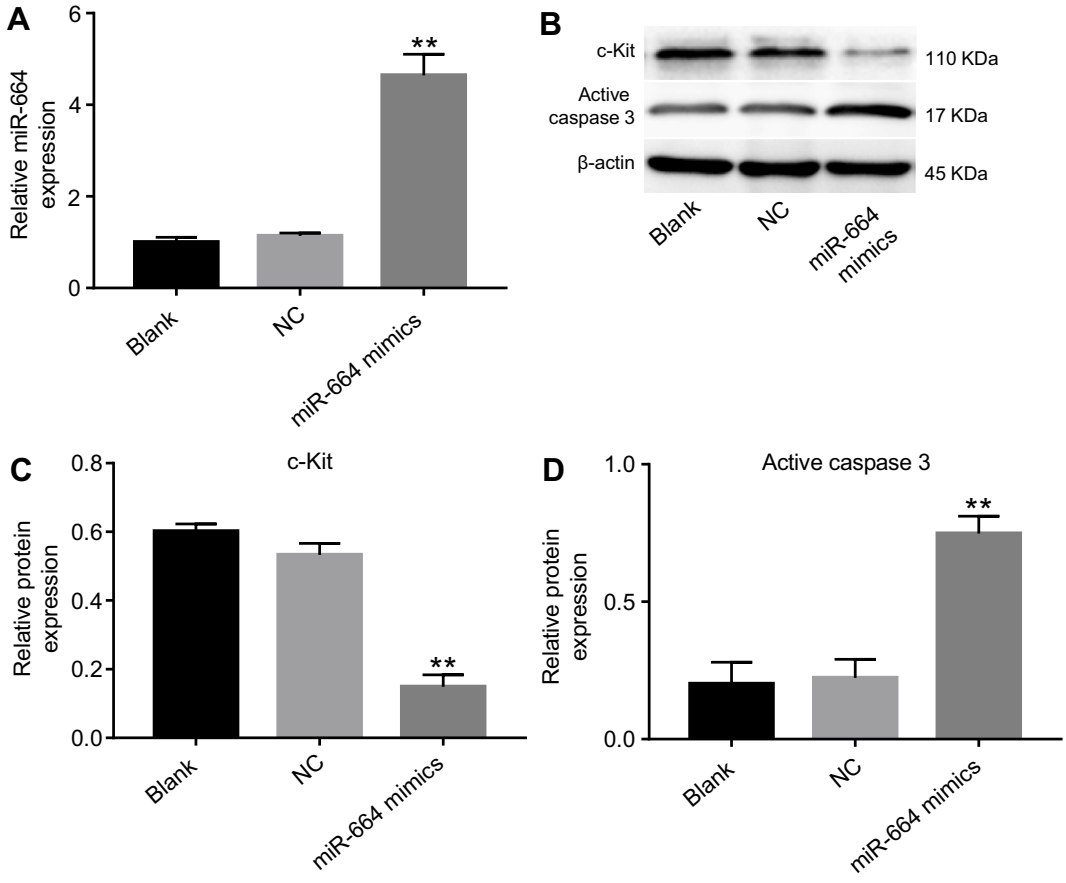


**Figure 6** MiR-664 mimics exhibited antitumor effects via induction apoptosis in vivo. (**A**) The level of miR-664 in tumor tissues was detected with qRT-PCR. (**B**) The expressions of c-Kit and active caspase 3 in tumor tissues were analyzed by Western blotting. (**C**) The expression of c-Kit was quantified by normalizing to β-actin. (**D**) The expression of active caspase 3 was quantified by normalizing to β-actin. ***P*<0.01 vs NC group.

the NC group (Figure 6B–D). All these results suggested that miR-664 exhibited antitumor effects via induction apoptosis in vivo.

## Discussion

Dysregulation of miRNAs may exhibit tumorigenic or tumor-suppressing effects by mediating target genes.[25,26] Recently, studies indicated that miR-664 exhibited differential expression in different human cancers.[17,27] Zhang et al indicated that low expression of miR-664 was associated with lower survival in cervical cancer.[28] In this study, the level of miR-664 was downregulated in human cervical cancer tissues, which was consistent with a previous study.[18] In addition, our results indicated that miR-664 mimics induced apoptosis of cervical cancer cells via increasing the levels of Bax and active caspase 3. However, miR-664 was upregulated in patients with lung cancer, which could enhance cell proliferation and inhibit apoptosis in lung cancer cells.[16,29] The difference between our result and previous studies might be the different types of cancers. The connection between miR-664 and human cancers is complicated, the specific pathogenesis needs further studying.

Several targets of miR-664, including SOX7 and FOXO4 have been identified in present years.[17,30] To investigate the mechanisms underlying the antitumor effect of miR-664 on cervical cancer, the potential binding genes of miR-664 were investigated by bioinformatics analysis. In this study, we found that c-*Kit* gene was the potential target gene of miR-664, which plays a vital role in tumor growth.[31] Meanwhile, the data of dual-luciferase reporter assay confirmed that *c-Kit* was the direct target of miR-664 in cervical cancer. Moreover, the protein level of c-Kit could be regulated by miR-664 mimics in vitro and in vivo. Franceschi et al found that overexpression of c-Kit promoted the proliferation in thyroid cancer cells.[32] C-Kit could mediate tumor-initiating capacity of ovarian cancer cells through activation of Wnt/β-catenin pathway.[33] Previous studies indicated that c-Kit could regulate the expression of the Wnt target gene Cyclin D1 and c-Myc in leukemia.[34] Our results demonstrated that overexpression of miR-664 inhibited proliferation and induced apoptosis via decreasing the expression of c-Kit, Cyclin D1 and c-Myc, which was consistent with the previous studies. Taken together, the underlying mechanism might be that miR-664 mimics suppressed the growth of cervical cancer cells through targeting c-Kit and inhibiting the levels of Wnt target gene Cyclin D1 and c-Myc. However, the precise function and mechanism of miR-664 in cervical cancer need further investigation.

## Conclusion

In the present study, we found that miR-664 mimics could inhibit the proliferation and migration of cervical cancer cells through targeting c-Kit in vitro and in vivo. Therefore, miR-664 might be a potential therapeutic target for the treatment of patients with cervical cancer.

## Acknowledgment

The study was funded by the National Natural Science Foundation of China (81571395, 81671408, 81771531, 81871129).

## Disclosure

The authors report no conflicts of interest in this work.

## References

1. Parkin DM, Bray F, Ferlay J, Pisani P. Estimating the world cancer burden: Globocan 2000. *Int J Cancer*. 2001;94(2):153–156.
2. Granados Lopez AJ, Lopez JA. Multistep model of cervical cancer: participation of miRNAs and coding genes. *Int J Mol Sci*. 2014;15(9):15700–15733. doi:10.3390/ijms150915700
3. de Freitas AC, Gomes Leitao Mda C, Coimbra EC. Prospects of molecularly-targeted therapies for cervical cancer treatment. *Curr Drug Targets*. 2015;16(1):77–91.
4. Shishodia G, Verma G, Das BC, Bharti AC. miRNA as viral transcription tuners in HPV-mediated cervical carcinogenesis. *Front Biosci (Schol Ed)*. 2018;10:21–47.
5. Filippeschi M, Moncini I, Bianchi B, Florio P. What kind of surgery for cervical carcinoma? *G Chir*. 2012;33(4):139–146.
6. Morales S, Monzo M, Navarro A. Epigenetic regulation mechanisms of microRNA expression. *Biomol Concepts*. 2017;8(5–6):203–212. doi:10.1515/bmc-2017-0024
7. McAnena P, Tanriverdi K, Curran C, et al. Circulating microRNAs miR-331 and miR-195 differentiate local luminal a from metastatic breast cancer. *BMC Cancer*. 2019;19(1):436. doi:10.1186/s12885-019-5636-y
8. Drusco A, Croce CM. MicroRNAs and cancer: a long story for short RNAs. *Adv Cancer Res*. 2017;135:1–24. doi:10.1016/bs.acr.2017.06.005
9. Fang Z, Rajewsky N. The impact of miRNA target sites in coding sequences and in 3'UTRs. *PLoS One*. 2011;6(3):e18067. doi:10.1371/journal.pone.0018067
10. Xian X, Tang L, Wu C, Huang L. miR-23b-3p and miR-130a-5p affect cell growth, migration and invasion by targeting CB1R via the Wnt/beta-catenin signaling pathway in gastric carcinoma. *Onco Targets Ther*. 2018;11:7503–7512. doi:10.2147/OTT.S181706
11. Kan X, Sun Y, Lu J, et al. Coinhibition of miRNA21 and miRNA221 induces apoptosis by enhancing the p53mediated expression of proapoptotic miRNAs in laryngeal squamous cell carcinoma. *Mol Med Rep*. 2016;13(5):4315–4320. doi:10.3892/mmr.2016.5048
12. Yin XZ, Zhao DM, Zhang GX, Liu L. Effect of miRNA-203 on cervical cancer cells and its underlying mechanism. *Genet Mol Res*. 2016;15(3). doi:10.4238/gmr.15038680
13. Li C, Jia L, Yu Y, Jin L. Lactic acid induced microRNA-744 enhances motility of SiHa cervical cancer cells through targeting ARHGAP5. *Chem Biol Interact*. 2018;298:86–95. doi:10.1016/j.cbi.2018.10.027
14. Fiala O, Pitule P, Hosek P, et al. The association of miR-126-3p, miR-126-5p and miR-664-3p expression profiles with outcomes of patients with metastatic colorectal cancer treated with bevacizumab. *Tumour Biol*. 2017;39(7):1010428317709283. doi:10.1177/1010428317709283

15. Lee BP, Buric I, George-Pandeth A, et al. MicroRNAs miR-203-3p, miR-664-3p and miR-708-5p are associated with median strain lifespan in mice. *Sci Rep*. 2017;7:44620. doi:10.1038/srep44620
16. Zhu X, Ju S, Yuan F, et al. microRNA-664 enhances proliferation, migration and invasion of lung cancer cells. *Exp Ther Med*. 2017;13(6):3555–3562. doi:10.3892/etm.2017.4433
17. Bao Y, Chen B, Wu Q, et al. Overexpression of miR-664 is associated with enhanced osteosarcoma cell migration and invasion ability via targeting SOX7. *Clin Exp Med*. 2017;17(1):51–58. doi:10.1007/s10238-015-0398-6
18. Yang Y, Liu H, Wang X, Chen L. Up-regulation of microRNA-664 inhibits cell growth and increases cisplatin sensitivity in cervical cancer. *Int J Clin Exp Med*. 2015;8(10):18123–18129.
19. Majumder S, Brown K, Qiu FH, Besmer P. c-kit protein, a transmembrane kinase: identification in tissues and characterization. *Mol Cell Biol*. 1988;8(11):4896–4903. doi:10.1128/mcb.8.11.4896
20. Zou T, Gao L, Zeng Y, et al. Organoid-derived C-Kit(+)/SSEA4(-) human retinal progenitor cells promote a protective retinal microenvironment during transplantation in rodents. *Nat Commun*. 2019;10(1):1205. doi:10.1038/s41467-019-08961-0
21. Stankov K, Popovic S, Mikov M. C-KIT signaling in cancer treatment. *Curr Pharm Des*. 2014;20(17):2849–2880.
22. Kellner J, Wallace C, Liu B, Li Z. Definition of a multiple myeloma progenitor population in mice driven by enforced expression of XBP1s. *JCI Insight*. 2019;4(7). doi:10.1172/jci.insight.122686
23. Aguilar C, Aguilar C, Lopez-Marure R, Jimenez-Sanchez A, Rocha-Zavaleta L. Co-stimulation with stem cell factor and erythropoietin enhances migration of c-Kit expressing cervical cancer cells through the sustained activation of ERK1/2. *Mol Med Rep*. 2014;9(5):1895–1902. doi:10.3892/mmr.2014.2044
24. Li XY, Wang X. The role of human cervical cancer oncogene in cancer progression. *Int J Clin Exp Med*. 2015;8(6):8363–8368.
25. Schickel R, Boyerinas B, Park SM, Peter ME. MicroRNAs: key players in the immune system, differentiation, tumorigenesis and cell death. *Oncogene*. 2008;27(45):5959–5974. doi:10.1038/onc.2008.274
26. Zhang B, Pan X, Cobb GP, Anderson TA. microRNAs as oncogenes and tumor suppressors. *Dev Biol*. 2007;302(1):1–12. doi:10.1016/j.ydbio.2006.08.028
27. Ding Z, Jian S, Peng X, et al. Loss of MiR-664 expression enhances cutaneous malignant melanoma proliferation by upregulating PLP2. *Medicine*. 2015;94(33):e1327. doi:10.1097/MD.0000000000000874
28. Zhang YX, Qin LL, Yang SY. Down-regulation of miR-664 in cervical cancer is associated with lower overall survival. *Eur Rev Med Pharmacol Sci*. 2016;20(9):1740–1744.
29. Lu Y, Govindan R, Wang L, et al. MicroRNA profiling and prediction of recurrence/relapse-free survival in stage I lung cancer. *Carcinogenesis*. 2012;33(5):1046–1054. doi:10.1093/carcin/bgs100
30. Chen B, Bao Y, Chen X, et al. Mir-664 promotes osteosarcoma cells proliferation via downregulating of FOXO4. *Biomed Pharmacother*. 2015;75:1–7. doi:10.1016/j.biopha.2015.08.012
31. Caceres-Cortes JR. A potent anti-carcinoma and anti-acute myeloblastic leukemia agent, AG490. *Anticancer Agents Med Chem*. 2008;8(7):717–722.
32. Franceschi S, Lessi F, Panebianco F, et al. Loss of c-KIT expression in thyroid cancer cells. *PLoS One*. 2017;12(3):e0173913. doi:10.1371/journal.pone.0173913
33. Chau WK, Ip CK, Mak AS, Lai HC, Wong AS. c-Kit mediates chemoresistance and tumor-initiating capacity of ovarian cancer cells through activation of Wnt/beta-catenin-ATP-binding cassette G2 signaling. *Oncogene*. 2013;32(22):2767–2781. doi:10.1038/onc.2012.290
34. Kajiguchi T, Lee S, Lee MJ, Trepel JB, Neckers L. KIT regulates tyrosine phosphorylation and nuclear localization of beta-catenin in mast cell leukemia. *Leuk Res*. 2008;32(5):761–770. doi:10.1016/j.leukres.2007.08.023